IEEE Control Systems Letters paper presented at
2024 IEEE 63rd Conference on Decision and Control (CDC)
December 16-19, 2024. MiCo, Milan, Italy

Prescribed-time Reach-Avoid-Stay Specifications for Unknown Systems: A Spatiotemporal Tubes Approach

Ratnangshu Das and Pushpak Jagtap

Abstract— **The paper considers controller synthesis problems for control-affine nonlinear systems with unknown dynamics, aiming to fulfil reach-avoid-stay specifications in a prescribed time. The research's primary aim is to devise a closed-form, approximation-free control strategy that ensures the system's trajectory reaches a target set, avoids an unsafe set, and complies with state constraints. To address this challenge, the paper introduces a spatiotemporal tube framework that encapsulates both reaching and avoiding requirements via reachability tubes and a circumvent function, respectively. Following this, the paper presents the control strategy and validates its effectiveness through a robot navigation case study.**

I. Introduction

In recent years, the study of reach-avoid-stay (RAS) specifications [1] has become increasingly relevant for enhancing safety and reliability in autonomous systems. These specifications are pivotal in ensuring that an autonomous system's state trajectory reaches a desired target set from a specific initial set and avoids any unsafe set while complying with state constraints. Developing controllers that meet RAS specifications is crucial as they form the foundation for more complex task specifications [2], [3] and are instrumental in designing robust control strategies for safety-critical scenarios, like path planning and motion planning.

Adopting formal languages for specifying complex tasks has led to the rise of symbolic control [4] as a powerful tool. Notably, SCOTS [5] has gained significant attention for its use of abstraction techniques to model system dynamics symbolically and thereby compute control strategies with formal guarantees. Moreover, advancements in computational methods, such as a fixed-point algorithm [6] for reach-avoid-stay controller synthesis, have improved upon traditional abstraction-based methods. Enhancements in the scalability of symbolic control for multi-agent systems have also been achieved by utilizing barrier certificates [7]. Nonetheless, these methods still face the challenge of the so-called curse of dimensionality.

In contrast, nonlinear control methods, such as barrier-based control [8], provide formal safety and stability guarantees without the need for discretizing the state space. The authors in [9], [10] have demonstrated implementing control (Lyapunov-)barrier functions for controller synthesis to meet RAS specifications. These approaches, however, depend on optimization-based solutions, which increase computational demands, particularly for larger, higher-dimensional systems.

The funnel-based control approach [11] [12], on the other hand, offers a closed-loop control to meet specific tracking performance. This approach is computationally more tractable and has been applied successfully in numerous scenarios [13], ranging from tracking control problems in unknown nonlinear systems [14] to managing multi-agent systems with complex tasks [15]. Moreover, as the feedback control algorithm dynamically adjusts the system's trajectory to guide it toward the target, it has been effective in enforcing reachability specifications [16], [3].

Yet, addressing nonconvex specifications, such as obstacle avoidance [17], through this technique remains a significant challenge. Some studies [18] have described a two-step process involving trajectory creation through path-planning algorithms and then applying funnel-based feedback control. However, separating the trajectory planning from funnels could compromise avoidance constraints under disturbances.

In our prior work [19], we demonstrated skipping the trajectory generation step by leveraging the funnel functions' ability to navigate around unsafe sets. In this context, we introduced the circumvent function to define the avoid specifications. The primary challenges identified include the necessity for knowledge of system dynamics, vulnerability to disturbances, longer computational times, and the inability to satisfy prescribed time requirements.

To overcome these issues, we present an alternative to the traditional funnel function in this study. The literature has proposed various alternatives to funnel functions, designed to address particular issues, such as eliminating dependence on initial conditions [20], ensuring finite-time convergence [21], and minimizing overshoot [22]. As a novel solution, the paper introduces a spatiotemporal tube framework that simultaneously captures reach and avoid specifications through continuously differentiable time-varying tube functions and circumvent functions, respectively, along with guaranteeing prescribed time satisfaction. Subsequently, we formulate an approximation-free closed-form control law that ensures the system's trajectory remains within these tubes, thereby achieving prescribed-time RAS objectives. The effectiveness of the proposed approach is showcased through a case study.

II. Preliminaries and Problem Formulation

Notations: The symbols $\mathbb{N}$, $\mathbb{R}$, $\mathbb{R}^+$, and $\mathbb{R}_0^+$ denote the set of natural, real, positive real, and nonnegative real numbers, respectively. We use $\mathbb{R}^{n\times m}$ to denote a vector space of real matrices with n rows and m columns. To represent a column

This work was supported in parts by the SERB Start-up Research Grant, the ARTPARK, and the CSR Grant by Siemens.

R. Das and P. Jagtap are with the Robert Bosch Centre for Cyber-Physical Systems, IISc, Bangalore, India {ratnangshud,pushpak}@iisc.ac.in

vector with n rows, we use $\mathbb{R}^n$. We represent the Euclidean norm using $\|\cdot\|$. For $a, b \in \mathbb{R}$ and $a < b$, we use (a, b) to represent open interval in $\mathbb{R}$. For $a, b \in \mathbb{N}$ and $a \leq b$, we use $[a; b]$ to denote close interval in $\mathbb{N}$. To denote a vector $x \in \mathbb{R}^n$ with entries $x_1, \ldots, x_n$, we use $[x_1, \ldots, x_n]^\top$, where $x_i \in \mathbb{R}, i \in [1; n]$ denotes i-th element of vector $x \in \mathbb{R}^n$. We use I_n to denote identity matrix in $\mathbb{R}^{n \times n}$. A diagonal matrix in $\mathbb{R}^{n \times n}$ with diagonal entries $d_1, \ldots, d_n$ is denoted by $\mathsf{diag}(d_1, \ldots, d_n)$. Given $N \in \mathbb{N}$ sets $\mathbf{X}_i$, $i \in [1; N]$, the Cartesian product of the sets is given by $\mathbf{X} = \prod_{i \in [1;N]} \mathbf{X}_i := \{(x_1, \ldots, x_N) | x_i \in \mathbf{X}_i, i \in [1; N]\}$. Consider a set $\mathbf{X}_a \subset \mathbb{R}^n$, its projection on ith dimension, where $i \in [1; n]$, is given by an interval $[\underline{\mathbf{X}}_{ai}, \overline{\mathbf{X}}_{ai}] \subset \mathbb{R}$, where $\underline{\mathbf{X}}_{ai} := \min\{x_i \in \mathbb{R} \mid [x_1 \ldots, x_n] \in \mathbf{X}_a\}$ and $\overline{\mathbf{X}}_{ai} := \max\{x_i \in \mathbb{R} \mid [x_1, \ldots, x_n] \in \mathbf{X}_a\}$. We further define the hyper-rectangle $[\![\mathbf{X}_a]\!] = \prod_{i=[1;n]} [\underline{\mathbf{X}}_{ai}, \overline{\mathbf{X}}_{ai}]$. We denote the empty set by $\emptyset$. The space of bounded continuous functions is denoted by $\mathcal{C}$. Given a compact set $\mathbf{X}$, $int(\mathbf{X})$ represents the interior of the set. $\overline{\max}$ and $\overline{\min}$ are smooth approximations of the non-smooth $\max$ and $\min$ functions, defined as, $\overline{\max}(a, b) \approx \frac{1}{\nu} \ln(\mathsf{e}^{\nu a} + \mathsf{e}^{\nu b})$ and $\overline{\min}(a, b) \approx -\frac{1}{\nu} \ln(\mathsf{e}^{-\nu a} + \mathsf{e}^{-\nu b})$, respectively.

A. System Definition

Consider the following control-affine nonlinear system:

$$\mathcal{S} : \dot{x} = f(x) + g(x)u + w, \tag{1}$$

where $x(t) = [x_1(t), \ldots, x_n(t)]^\top \in \mathbf{X} \subset \mathbb{R}^n$ and $u(t) \in \mathbb{R}^n$ are the state and control input vectors, respectively. $w(t) \in \mathbb{W} \subset \mathbb{R}^n$ denotes unknown bounded disturbance. The state space of the system is defined by the closed and connected set $\mathbf{X}$.

Assumption 1: The functions $f : \mathbf{X} \to \mathbb{R}^n$ and $g : \mathbf{X} \to \mathbb{R}^{n \times n}$ in (1) are unknown and locally Lipschitz.

Assumption 2: ([11], [23]) The symmetric components of $g(x)$ denoted by $g_s(x) = \frac{g(x) + g(x)^\top}{2}$ are uniformly sign definite with known signs for all $x \in \mathbf{X}$. Without loss of generality, we assume $g_s(x)$ is uniformly positive definite, i.e., there exists a constant $\underline{g} \in \mathbb{R}^+$:

$$0 < \underline{g} \leq \lambda_{\min}(g_s(x)), \forall x \in \mathbf{X},$$

where $\lambda_{\min}(\cdot)$ is the smallest eigenvalue of the matrix.

B. Problem Formulation

Let $\mathbf{U} = \bigcup_{j \in [1; n_u]} \mathcal{U}^j \subset \mathbf{X}$ be an unsafe set, where $n_u \in \mathbb{R}_0^+$ and $\mathcal{U}^j \subset \mathbf{X}$ is assumed to be compact and convex. Note that, in general, $\mathbf{U}$ can be nonconvex and disconnected. The compact connected sets $\mathbf{X}_0 \subset \mathbf{X} \setminus \mathbf{U}$ and $\mathbf{T} \subset \mathbf{X} \setminus \mathbf{U}$ represent the initial and target sets, respectively. Further, if $\mathbf{X}$ is of any arbitrary shape, we redefine the state space as $\hat{\mathbf{X}} := [\![\mathbf{X}]\!] = \prod_{i \in [1;n]} [\underline{\mathbf{X}}_i, \overline{\mathbf{X}}_i]$ and expand the unsafe set as $\hat{\mathbf{U}} = \mathbf{U} \cup ([\![\mathbf{X}]\!] \setminus \mathbf{X})$. We consider a prescribed-time reach-avoid-stay problem defined in Definition 2.1.

Definition 2.1 (Prescribed-time Reach-Avoid-Stay Task): Given a state-space $\mathbf{X}$, let $\mathbf{U}$ be an unsafe set, $\mathbf{X}_0 \in \mathbf{X} \setminus \mathbf{U}$ be an initial set, and $\mathbf{T} \in \mathbf{X} \setminus \mathbf{U}$ be a target set. For a given initial position $x(0) \in \mathbf{X}_0$, there exists $t \in [0, t_c]$, such that, $x(t) \in \mathbf{T}$ and for all $s \in [0, t_c], x(s) \in \mathbf{X} \setminus \mathbf{U}$, where $t_c \in \mathbb{R}^+$ is the prescribed-time.

Problem 2.2: Given the system $\mathcal{S}$ in (1) satisfying assumptions 1 and 2, design a *closed-form* controller to ensure the satisfaction of prescribed-time reach-avoid-stay specifications in Definition 2.1.

III. Designing Spatiotemporal Tubes

The spatiotemporal tubes are generated in three steps. First, we design reachability tubes that take the system trajectory from $\mathbf{X}_0$ to the target $\mathbf{T}$. Second, we introduce a circumvent function to avoid the unsafe set $\mathbf{U}$. Finally, adjusting the tube dynamically around the unsafe region, the spatiotemporal tubes capture RAS constraints.

A. Reachability Tubes

In this section, we formulate reachability tubes, guaranteeing that the system's trajectory starting from $x(0) \in \mathbf{X}_0$ enters target set $\mathbf{T}$ in finite time t_c.

We define $\hat{\mathbf{X}}_0$ as a hyper-rectangle around the initial state $x(0) \in int(\mathbf{X}_0)$ and subset of the initial set $\mathbf{X}_0$:

$$\hat{\mathbf{X}}_0 := \prod_{i=[1;n]} [x_i(0) - d_{0,i}, x_i(0) + d_{0,i}] \subset \mathbf{X}_0, \tag{2}$$

where $d_{0,i} \in \mathbb{R}^+$ determines the size of $\hat{\mathbf{X}}_0$. We further choose a point $\eta = [\eta_1, \ldots, \eta_n]^\top \in int(\mathbf{T})$, and define a hyper-rectangle $\hat{\mathbf{T}}$ around η and subset of the target set $\mathbf{T}$:

$$\hat{\mathbf{T}} := \prod_{i=[1;n]} [\eta_i - d_{T,i}, \eta_i + d_{T,i}] \subset \mathbf{T}, \tag{3}$$

where $d_{T,i} \in \mathbb{R}^+$ determines the size of $\hat{\mathbf{T}}$.

Now, the reachability tube constraints are defined as $\rho_L(t) = [\rho_{1,L}(t), \ldots, \rho_{n,L}(t)]^\top$ and $\rho_U(t) = [\rho_{1,U}(t), \ldots, \rho_{n,U}(t)]^\top$, where $\rho_{i,L}(t)$ and $\rho_{i,U}(t)$ are the continuously differentiable tube functions representing the lower and upper boundaries of the tube in ith dimension and are defined as:

$$\rho_{i,L}(t) = \begin{cases} (\underline{\hat{\mathbf{T}}}_i - \underline{\hat{\mathbf{X}}}_{0,i}) \tanh \frac{t}{t_c - t} + \underline{\hat{\mathbf{X}}}_{0,i}, & \text{if } t < t_c \\ \underline{\hat{\mathbf{T}}}_i, & \text{if } t \geq t_c \end{cases}$$
$$\rho_{i,U}(t) = \begin{cases} (\overline{\hat{\mathbf{T}}}_i - \overline{\hat{\mathbf{X}}}_{0,i}) \tanh \frac{t}{t_c - t} + \overline{\hat{\mathbf{X}}}_{0,i}, & \text{if } t < t_c \\ \overline{\hat{\mathbf{T}}}_i, & \text{if } t \geq t_c. \end{cases} \tag{4}$$

Figure 1(b) illustrates the reachability tube design.

B. Circumvent Function

Consider an unsafe set $\mathbf{U} = \bigcup_{j \in [1; n_u]} \mathcal{U}^j \subset \mathbf{X}$, adhering to Assumption 3. We propose to enforce the avoid specifications through a circumvent function $\beta^j : \mathbb{R}_0^+ \to \mathbb{R}^n$, $j \in [1; n_u], n_u \in \mathbb{R}_0^+$.

Assumption 3: There exists at least one dimension $k_i \in [1; n]$ where $\hat{\mathbf{X}}_0$ and unsafe sets $\mathcal{U}^j$ does not overlap for all $j \in [1; n_u]$, i.e., $\exists k_i \in [1; n]$ such that, $[\underline{\hat{\mathbf{X}}}_{0,k_i}, \overline{\hat{\mathbf{X}}}_{0,k_i}] \cap [\underline{\mathcal{U}}^j_{k_i}, \overline{\mathcal{U}}^j_{k_i}] = \emptyset, \forall j \in [1; n_u]$. And there exists at least one dimension $k_T \in [1; n]$ where $\hat{\mathbf{T}}$ and the unsafe sets $\mathcal{U}^j$ does

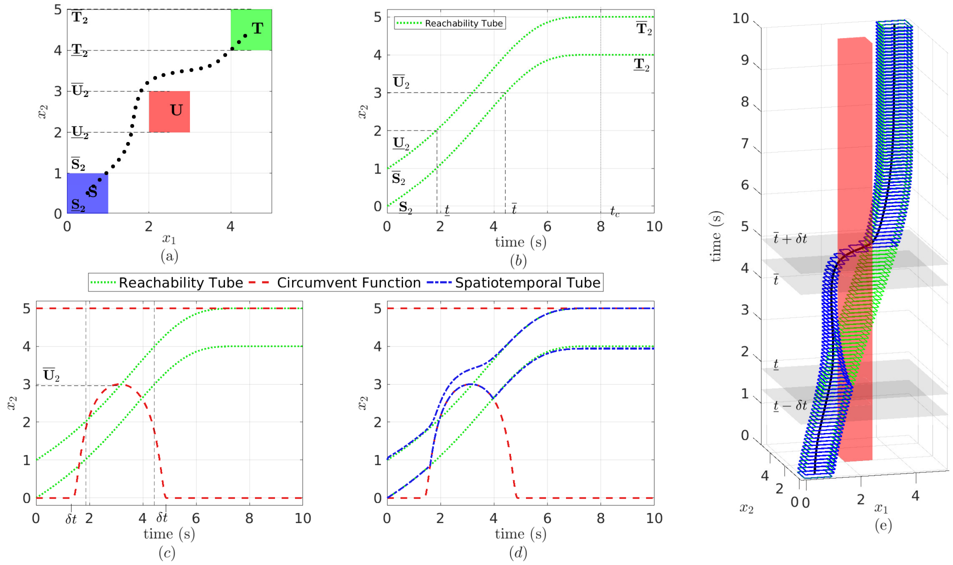

t

Fig. 1: An example of Spatiotemporal tube design for a two-dimensional system $x(t) = [x_1(t), x_2(t)]^\top$, assigned the task: "*Starting from* **S**, *reach* **T**, *while avoiding* **U**, *within* $t = 8s$". (a) State space and the controlled trajectory (black dotted line). (b) Reachability tube Design (c) Introduction of the circumvent function. (d) Spatiotemporal tube adapted around the circumvent function. (e) 3D visualization of spatiotemporal tubes with time as the third dimension.

not overlap for all $j \in [1; n_u]$, i.e., $\exists k_T \in [1; n]$ such that, $[\underline{\mathbf{T}}_{0,k_T}, \overline{\mathbf{T}}_{0,k_T}] \cap [\underline{\mathcal{U}}^j_{k_T}, \overline{\mathcal{U}}^j_{k_T}] = \emptyset, \forall j \in [1; n_u]$.

Remark 3.1: Note that Assumption 3 can be relaxed by splitting the unsafe set. In Figure 2 while $\mathcal{U} = \mathcal{U}_1 \cup \mathcal{U}_2$ violates the assumption, splitting it into $\mathcal{U}_1$ and $\mathcal{U}_2$ resolves the issue. Details on splitting methods are beyond the scope of this paper.

Next, we obtain the time range $[\underline{t}^j, \overline{t}^j]$ over which the tube intersects with the jth unsafe set $\mathcal{U}^j$, and is given by,

$$a^j_{1,i} = tanh^{-1}\left(\frac{\underline{\mathcal{U}}^j_i - \hat{\underline{\mathbf{X}}}_{0,i}}{\hat{\underline{\mathbf{T}}}_i - \hat{\underline{\mathbf{X}}}_{0,i}}\right), \; a^j_{2,i} = tanh^{-1}\left(\frac{\overline{\mathcal{U}}^j_i - \hat{\underline{\mathbf{X}}}_{0,i}}{\hat{\underline{\mathbf{T}}}_i - \hat{\underline{\mathbf{X}}}_{0,i}}\right),$$
$$a^j_{3,i} = tanh^{-1}\left(\frac{\underline{\mathcal{U}}^j_i - \hat{\overline{\mathbf{X}}}_{0,i}}{\hat{\overline{\mathbf{T}}}_i - \hat{\overline{\mathbf{X}}}_{0,i}}\right), \; a^j_{4,i} = tanh^{-1}\left(\frac{\overline{\mathcal{U}}^j_i - \hat{\overline{\mathbf{X}}}_{0,i}}{\hat{\overline{\mathbf{T}}}_i - \hat{\overline{\mathbf{X}}}_{0,i}}\right),$$
$$\overline{a}_i = \left\{\frac{a^j_{1,i}}{1 + a^j_{1,i}}, \frac{a^j_{2,i}}{1 + a^j_{2,i}}, \frac{a^j_{3,i}}{1 + a^j_{3,i}}, \frac{a^j_{4,i}}{1 + a^j_{4,i}}\right\},$$
$$\underline{t}^j = (\max_{i \in [1;n]} \min \overline{a}_i) t_c, \; \overline{t}^j = (\min_{i \in [1;n]} \max \overline{a}_i) t_c. \tag{5}$$

Further, note that if the system's trajectory enters the unsafe zone $\mathcal{U}^j$, then $\exists t \in \mathbb{R}^+$, such that $x_i(t) \cap [\underline{\mathcal{U}}^j_i, \overline{\mathcal{U}}^j_i] \neq \emptyset, \forall i \in [1; n]$. Hence, to satisfy the avoid specification, it is sufficient to introduce the circumvent function only in one dimension i^j, given by

$$i^j_1 = argmax_{i \in [1;n]} \min \overline{a}_i, \; i^j_2 = argmin_{i \in [1;n]} \max \overline{a}_i,$$
$$i^j = argmin_{k = \{i^j_1, i^j_2\}} (\max \overline{a}_k - \min \overline{a}_k). \tag{6}$$

We can choose to modify either the upper or lower constraint boundary of the tube. However, if $\underline{\mathcal{U}}^j_i = \underline{\mathbf{X}}_i$ or $\overline{\mathcal{U}}^j_i = \overline{\mathbf{X}}_i$, the circumvent function must be introduced in the lower or upper constraint boundary, respectively (this is analogous to a wall-shaped obstacle scenario with no space between the state space boundary and the obstacle at one end). In other cases, we randomly select between the two options.

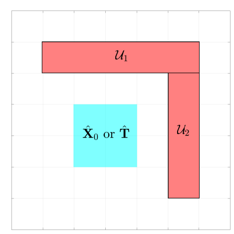

Fig. 2: A two dimensional state space demonstrating relaxation of Assumption 3.

We define the circumvent function on the lower constraint boundary for $i = i^j$ as:

$$\underline{\beta}^j_i(t) = \begin{cases} B^j \mathrm{e}^{\frac{-k^j (t - m^j)^2}{(r^j)^2 - (t - m^j)^2}} + \underline{\mathbf{X}}_i, & \forall t \in T_{act}, \\ \underline{\mathbf{X}}_i, & \forall t \in \mathbb{R}^+ \setminus T_{act}, \end{cases} \tag{7}$$

where $B^j = \overline{\mathcal{U}}^j_i - \underline{\mathbf{X}}_i + \delta B$, $m^j := \frac{\underline{t}^j + \overline{t}^j}{2}$, $r^j := \frac{\underline{t}^j - \overline{t}^j}{2}$. The function is active in the time range $T_{act} = [\underline{t}^j, \overline{t}^j]$ when the system trajectory avoids $\mathcal{U}^j$. The $\delta B \in \mathbb{R}^+$ governs how far from $\mathcal{U}^j$ should the trajectory stay clear. The small positive constant $k^j \in R^+$ determines the smoothness of the circumvent function. Similarly, we define a circumvent on the upper constraint boundary for $i = i^j$ as:

$$\overline{\beta}_i^j(t) = \begin{cases} -B^j \mathsf{e}^{\frac{-k^j\left(t-m^j\right)^2}{(r^j)^2-(t-m^j)^2}} + \overline{\mathbf{X}}_i, & \forall t \in T_{act} \\ \overline{\mathbf{X}}_i, & \forall t \in \mathbb{R}^+ \setminus T_{act} \end{cases} \quad (8)$$

with $B^j = \overline{\mathbf{X}}_i - \underline{\mathcal{U}}_i^j + \delta B$ and the rest is the same as above.

Combining the circumvent functions for all unsafe sets $\mathcal{U}^j$, we define the tube analog of avoid specification as a holistic circumvent function $\beta_i(t) = [\beta_{i,L}(t), \beta_{i,U}(t)]$ and $\beta(t) = [\beta_1(t), \ldots, \beta_n(t)]^\top$, where

$$\beta_{i,L}(t) = \max_{j=[1;n_u]} \underline{\beta}_i^j(t),\ \beta_{i,U}(t) = \min_{j=[1;n_u]} \overline{\beta}_i^j(t). \quad (9)$$

The circumvent function is illustrated in Figure 1(c).

Remark 3.2: Note, that the definition of circumvent function (9) not only ensures *avoiding* the unsafe set $\mathbf{U}$, but also guarantees *staying* inside the state space $\prod_{i=[1;n]} \left[\underline{\mathbf{X}}_i, \overline{\mathbf{X}}_i\right]$.

C. Spatiotemporal Tube Design

We have expressed the prescribed-time reachability specification through the tube constraints $\rho_L(t)$ and $\rho_U(t)$ (4), and the avoid specification through the circumvent function $\beta(t)$ (9). To enforce PT-RAS specification, we propose an adaptive framework, akin to [16], to modify the reachability tubes around the circumvent function. We define the following adaptive tube constraints:

$$\begin{aligned} \gamma_{i,L}(t) &:= \overline{\max}(\rho_{i,L}(t) - \alpha_{i,L}(t), \beta_{i,L}(t)), \\ \gamma_{i,U}(t) &:= \overline{\min}(\rho_{i,U}(t) + \alpha_{i,U}(t), \beta_{i,U}(t)), \end{aligned} \quad (10)$$

where a continuously differentiable update function $\alpha^\wr(t) = [\alpha_1^\wr(t), \ldots, \alpha_n^\wr(t)]^\top$ captures the modifications in the tubes. The symbol $\wr \in \{L, U\}$ indicate the upper (U) and lower (L) constraints, respectively. The adaptive law governing the dynamics of the update function is defined as:

$$\dot{\alpha}_i^\wr(t) = \frac{\theta_i^\wr(t)}{(\psi_i^\wr(t) + \alpha_i^\wr(t))^2} - \kappa\alpha_i^\wr(t),\ \alpha_i^\wr(0) = 0, \quad (11)$$

where $\wr \in \{L, U\}$, $\psi_i^L(t) = \beta_{i,U}(t) - \rho_{i,L}(t)$ and $\psi_i^U(t) = \rho_{i,U}(t) - \beta_{i,L}(t)$. When the reach-avoid specifications conflict with a tolerance of $\mu \in \mathbb{R}^+$, $\theta_i^\wr(t) = \theta_o(1 - \mathsf{sign}(\psi_i^\wr(t) - \mu)), \theta_o \in \mathbb{R}^+, \wr \in \{L, U\}$, acts as a trigger, activating the first part of the update function. When the conflict is resolved, $\alpha^\wr$ exponentially decays back to 0 with a decay rate $\kappa \in \mathbb{R}^+$. The non-smooth $\mathsf{sign}(\cdot)$ function is approximated by the smooth function $\tanh(\cdot)$. An illustration of the designed spatiotemporal tube is shown in Figure 1(d).

Thus, we can enforce RAS specification by constraining the state trajectory within the spatiotemporal tubes (10) as:

$$\gamma_{i,L}(t) < x_i(t) < \gamma_{i,U}(t), \forall (t, i) \in \mathbb{R}^+ \times [1; n]. \quad (12)$$

Lemma 3.3: $\gamma_s(t), \dot{\gamma}_s(t), \gamma_d(t), \dot{\gamma}_d(t) \in \mathcal{C}$, where $\gamma_L = [\gamma_{1,L}, \ldots, \gamma_{n,L}]^\top$, $\gamma_U = [\gamma_{1,U}, \ldots, \gamma_{n,U}]^\top$, $\gamma_d = \mathsf{diag}(\gamma_{1,U} - \gamma_{1,L}, \ldots, \gamma_{n,U} - \gamma_{n,L})$, and $\gamma_s = \gamma_U + \gamma_L$.

Proof: The proof follows a similar approach to that of Lemma 4.2 in [19] and Lemma 1 in [16]. ∎

IV. Controller Design

In this section, utilizing the spatiotemporal tubes (10), we derive an *aproximation-free*, *closed-form* control law, similar to [12], to satisfy (12), thereby solving Problem 2.2.

Define the normalized error $e(x, t)$, the transformed error $\varepsilon(x, t)$ and the diagonal matrix $\xi(x, t)$ as

$$\begin{aligned} e(x, t) &= [e_1(x_1, t), \ldots, e_n(x_n, t)]^\top = \gamma_d^{-1}(t)\,(2x - \gamma_s(t)), \\ \varepsilon(x, t) &= \left[\ln\left(\frac{1 + e_1(x_1, t)}{1 - e_1(x_1, t)}\right), \ldots, \ln\left(\frac{1 + e_n(x_n, t)}{1 - e_n(x_n, t)}\right)\right]^\top, \\ \xi(x, t) &= 4\gamma_d^{-1}\left(I_n - e(x, t)e^\top(x, t)\right)^{-1}, \end{aligned}$$

where, $\gamma_s := [\gamma_{1,U} + \gamma_{1,L}, \ldots, \gamma_{n,U} + \gamma_{n,L}]^\top$ and $\gamma_d := \mathsf{diag}(\gamma_{1,d}, \ldots, \gamma_{n,d})$, with $\gamma_{i,d} = \gamma_{i,U} - \gamma_{i,L}$.

Theorem 4.1: Consider the nonlinear control-affine system $\mathcal{S}$ in (1). If the initial state $x(0)$ is within the spatiotemporal tubes, i.e., $\gamma_{i,L}(0) < x_i(0) < \gamma_{i,U}(0), \forall i \in [1; n]$, then the closed-form control strategy,

$$u(x, t) = -k\xi(x, t)\varepsilon(x, t), k \in \mathbb{R}^+, \quad (13)$$

will satisfy (12), thereby driving the state $x(t)$ to the target $\mathbf{T}$ in finite time t_c, while avoiding the unsafe set $\mathbf{U}$ and adhering to state constraints.

Proof: Differentiating the normalized error e w.r.t time and substituting the system dynamics (1) we get,

$$\dot{e} = \underbrace{2\gamma_d^{-1}(t)\left(f(x) + g(x)u + w - \frac{1}{2}\left(\dot{\gamma}_s(t) + \dot{\gamma}_d(t)e\right)\right)}_{h(t,e)},$$

where, $x = \frac{\gamma_d(t)e + \gamma_s(t)}{2}$. We also define the constraints for e through the open and bounded set $\mathbb{D} := (-1, 1)^n$.

Now, the proof proceeds in three steps. First, we show that there exists a maximal solution for the normalized error $e : [0, \tau_{\max}] \to \mathbb{D}$, which implies that $e(t)$ remains within $\mathbb{D}$ in the maximal time solution interval $[0, \tau_{\max})$. Next, we show that the proposed control law (13) constraints $e(t)$ to a compact subset of $\mathbb{D}$. Finally, we prove that $\tau_{\max}$ can be extended to ∞.

Step 1. Since the initial state $x(0)$ satisfies $\gamma_L(0) < x(0) < \gamma_U(0)$, the initial normalized error $e(0)$ is also within the constrained region $\mathbb{D}$. Further, the spatiotemporal tube functions $\gamma_L(t)$ and $\gamma_U(t)$ are bounded and continuously differentiable functions of time, the functions $f(x)$ and $g(x)$ are locally Lipschitz and the control law u is smooth over $\mathbb{D}$. As a consequence, $h(t, e)$ is bounded and continuously differentiable on t and locally Lipschitz on e over $\mathbb{D}$.

Therefore, according to [24, Theorem 54], there exists a maximal solution to the initial value problem $\dot{e} = h(t, e), e(0) \in \mathbb{D}$ on the time interval $[0, \tau_{\max})$ such that $e(t) \in \mathbb{D}, \forall t \in [0, \tau_{\max})$.

Step 2. Consider the following positive definite and radially unbounded Lyapunov function candidate: $V = \frac{1}{2}\varepsilon^\top\varepsilon$.

Differentiating V w.r.t. t and substituting $\dot{\varepsilon}$, $\dot{e}$, system dynamics (1), and the control strategy (13), we obtain:

$$
\begin{aligned}
\dot{V} &= \varepsilon^\top \dot{\varepsilon} = \varepsilon^\top 2\left(I_n - ee^\top\right)^{-1} \dot{e} \\
&= \varepsilon^\top \xi \left(\dot{x} - \frac{1}{2}(\dot{\gamma}_s + \dot{\gamma}_d e)\right) \\
&= \varepsilon^\top \xi \left(f(x) + g(x)u + w - \frac{1}{2}(\dot{\gamma}_s + \dot{\gamma}_d e)\right) \\
&= \varepsilon^\top \xi \left(f(x) - kg(x)\xi\varepsilon + w - \frac{1}{2}(\dot{\gamma}_s + \dot{\gamma}_d e)\right).
\end{aligned}
$$

Now, by Rayleigh-Ritz inequality and Assumption 2,

$$
\begin{aligned}
\underline{g}\|\varepsilon\|^2\|\xi\|^2 \le \lambda_{\min}(g_s(x))\|\varepsilon\|^2\|\xi\|^2 \le \varepsilon^\top \xi g(x)\xi\varepsilon, \\
-k\varepsilon^\top \xi g(x)\xi\varepsilon \le -k\underline{g}\|\varepsilon\|^2\|\xi\|^2 = k_g\|\varepsilon\|^2\|\xi\|^2.
\end{aligned}
$$

Therefore, $\dot{V} \le -k_g\|\varepsilon\|^2\|\xi\|^2 + \|\varepsilon\|\|\xi\|\|\Phi\|$, where $\Phi := f(x) + w - \frac{1}{2}\dot{\gamma}_s - \frac{1}{2}\dot{\gamma}_d e$. From Lemma 3.3, we know that $\dot{\gamma}_s$ and $\dot{\gamma}_d$ are bounded by construction. From step 1, we have $e(t) \in \mathbb{D}$ and consequently $x(t) \in (\gamma_L(t), \gamma_U(t))$. Thus, owing to the continuity of $f(x)$ and $g(x)$ and employing the extreme value theorem, we can infer $\|f(x)\|, \|g(x)\| < \infty$. Hence, $\|\Phi\| < \infty, \forall t \in [0, \tau_{max})$.

Now add and substract $k_g\theta \|\varepsilon\|^2 \|\xi\|^2$, where $\theta \in (0, 1)$.

$$
\begin{aligned}
\dot{V} &\le -k_g(1-\theta)\|\varepsilon\|^2\|\xi\|^2 - \|\varepsilon\|\|\xi\|\left(k_g\theta\|\varepsilon\|\|\xi\| - \|\Phi\|\right) \\
&\le -k_g(1-\theta)\|\varepsilon\|^2\|\xi\|^2, \forall k_g\theta\|\varepsilon\|\|\xi\| - \|\Phi\| \ge 0 \\
&\le -k_g(1-\theta)\|\varepsilon\|^2\|\xi\|^2, \forall \|\varepsilon\| \ge \frac{\|\Phi\|}{k_g\theta\|\xi\|}, \forall t \in [0, \tau_{\max}).
\end{aligned}
$$

Therefore, we can conclude that there exists a time-independent upper bound $\varepsilon^* \in \mathbb{R}_0^+$ to the transformed error ε, i.e., $\|\varepsilon\| \le \varepsilon^*, \forall t \in [0, \tau_{\max})$.

Consequently taking inverse logarithmic function,

$$
-1 < \frac{e_i^{-\varepsilon_i^*} - 1}{e_i^{-\varepsilon_i^*} + 1} =: e_{i,L} \le e_i \le e_{i,U} := \frac{e_i^{\varepsilon_i^*} - 1}{e_i^{\varepsilon_i^*} + 1} < 1,
$$

$\forall t \in [0, \tau_{\max})$, for $i \in [1; n]$. Therefore, by employing the control law (13), we can constrain e to a compact subset of $\mathbb{D}$ as: $e(t) \in [e_L, e_U] =: \mathbb{D}' \subset \mathbb{D}, \forall t \in [0, \tau_{\max})$ where, $e_L = [e_{1,L}, \ldots, e_{n,L}]^\top$ and $e_U = [e_{1,U}, \ldots, e_{n,U}]^\top$

Step 3. Finally, we prove $\tau_{\max}$ can be extended to ∞.

We know that $e(t) \in \mathbb{D}', \forall t \in [0, \tau_{\max})$, where $\mathbb{D}'$ is a non-empty compact subset of $\mathbb{D}$. However, if $\tau_{\max} < \infty$ then according to [24, Proposition C.3.6], $\exists t' \in [0, \tau_{\max})$ such that $e(t) \notin \mathbb{D}$. This leads to a contradiction! Hence, we conclude that $\tau_{\max}$ can be extended to ∞. In conclusion, the control strategy (13) guarantees the satisfaction of (12). ∎

Remark 4.2: Note that the closed-form time-dependent control law (13) is approximation-free and guarantees the satisfaction of RAS specifications for control affine systems with unknown dynamics. Additionally, if $g_s(x)$ is negative definite, k (in control law (13)) $\in \mathbb{R} \setminus \mathbb{R}_0^+$.

V. Case Study

Spatiotemporal tubes offer a closed-form solution for general RAS tasks. To illustrate the effectiveness of this approach, we consider a robot navigation problem using an omnidirectional robot defined as:

$$
\begin{bmatrix} \dot{x}_1 \\ \dot{x}_2 \\ \dot{x}_3 \end{bmatrix} = \begin{bmatrix} \cos x_3 & -\sin x_3 & 0 \\ \sin x_3 & \cos x_3 & 0 \\ 0 & 0 & 1 \end{bmatrix} \begin{bmatrix} v_1 \\ v_2 \\ \omega \end{bmatrix} + w(t), \tag{14}
$$

where the state vector $[x_1, x_2, x_3]^\top$ captures the robot's pose, $[v_1, v_2, \omega]^\top$ is the input velocity vector in the robot's frame, and w is an external disturbance. The robot operates in a 2D arena with multiple obstacles in the presence of unknown bounded external disturbance. Starting from three different initial sets $S_1 = [0, 0.5] \times [4.5, 5]$, $S_2 = [0, 0.5] \times [0, 0.5]$ and $S_3 = [4, 4.5] \times [0, 0.5]$, the aim is to reach a target set $T = [4.5, 5] \times [4.5, 5]$, while avoiding obstacles $O_1 = [1, 2] \times [4, 5]$, $O_2 = [2, 3] \times [2.5, 3.5]$, $O_3 = [1, 2] \times [0.5, 1.5]$, and $O_4 = [4, 5] \times [1.5, 2.5]$ and remaining inside the state space boundaries $[0, 5] \times [0, 5]$. The spatiotemporal tubes are shaped with the following parameters: $t_c = 9, \delta B = 0.2, k = 0.01, \theta_0 = 0.01, \kappa = 5$, and $\mu = 1$. Figure 3 depicts the simulation results with three different initial states.

The case study can also be solved using path planning and path-following algorithms. However, these algorithms have a moderate to high computation complexity and fail to provide any formal guarantee of solution quality. On the other hand, symbolic control techniques do provide formal guarantees at the cost of increased computation complexity. We ran tests in 500 arenas, randomly placing the obstacles at different locations, and compared the proposed spatiotemporal tube-based control approach against some state-of-the-art techniques presented in the literature. We used a computer with an Intel Core i7-11700 Processor and 16 GB RAM to run the simulations on MATLAB. Table I summarizes the findings, bringing forth the effectiveness of spatiotemporal tubes.

VI. Conclusion and Future Work

In this work, we consider a prescribed-time reach-avoid-stay control problem. Given an initial set, a target set, an unsafe set, and state constraints, we first proposed a spatiotemporal tube framework. We have then derived a closed-form control law guaranteeing that the state trajectories are constrained within the spatiotemporal tubes, enforcing prescribed-time reach-avoid-stay specifications. The feedback control law is approximation-free and works on control-affine systems with unknown dynamics. Finally, the efficacy of the proposed approach is demonstrated through a robot navigation case study, and the results are compared with those of other state-of-the-art algorithms in the literature.

Currently, our approach is limited to fully actuated systems as stated in Assumption 1. Future work will expand this to include underactuated control systems. Additionally, we plan to enhance the method's ability to meet reach-avoid specifications and address general specifications described using regular expressions. Our present control strategy cannot meet arbitrary input constraints, and we aim to develop solutions accommodating input constraints.

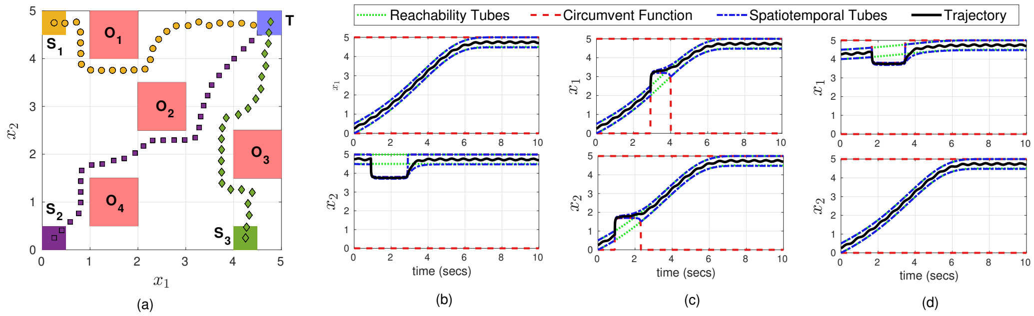

Fig. 3: Spatiotemporal tube-based control to satisfy RAS tasks for three different initial states starting from S_1, S_2 and S_3. (b), (c) and (d) The spatiotemporal tubes reaching T avoiding $O_1 \cup O_2 \cup O_3 \cup O_4$, starting from S_1, S_2, and S_3, respectively.

TABLE I: Comparing spatiotemporal tubes with classical algorithms

Algorithm	**Success Rate (%)**	**Computation Time (secs)**	**Formal Guarantees**	
A* [25] [26]	95.40	3.32	Optimality under certain conditions	For tracking, we need additional mechanisms such as PID, MPC, Funnel-based control, etc.
RRT* [25] [26]	97.40	10.57	Probabilistic completeness	
RL [27]	99.20	99.31	No formal guarantee	
Symbolic Control [5]	100.00	295.46	Formal guarantees under accurate modelling	
Spatiotemporal Tubes	100.00	0.02	Formal guarantees with unknown dynamics	

References

[1] Y. Meng, Y. Li, and J. Liu, "Control of nonlinear systems with reach-avoid-stay specifications: A Lyapunov-barrier approach with an application to the Moore-Greizer model," in *American Control Conference*, pp. 2284–2291, 2021.

[2] M. Kloetzer and C. Belta, "A fully automated framework for control of linear systems from temporal logic specifications," *IEEE Transactions on Automatic Control*, vol. 53, no. 1, pp. 287–297, 2008.

[3] P. Jagtap and D. V. Dimarogonas, "Controller synthesis against omega-regular specifications: A funnel-based control approach," *International Journal of Robust and Nonlinear Control*, 2024.

[4] P. Tabuada, *Verification and control of hybrid systems: a symbolic approach*. Springer Science and Business Media, 2009.

[5] M. Rungger and M. Zamani, "SCOTS: A tool for the synthesis of symbolic controllers," in *the 19th International Conference on Hybrid Systems: Computation and Control*, pp. 99–104, 2016.

[6] Y. Li and J. Liu, "Robustly complete synthesis of memoryless controllers for nonlinear systems with reach-and-stay specifications," *IEEE Transactions on Automatic Control*, vol. 66, no. 3, pp. 1199–1206, 2021.

[7] D. S. Sundarsingh, J. Bhagiya, J. Chatrola, A. Saoud, and P. Jagtap, "Controller synthesis for local and global specifications in multi-agent systems," in *The 62nd IEEE Conference on Decision and Control*, 2023.

[8] A. D. Ames, X. Xu, J. W. Grizzle, and P. Tabuada, "Control barrier function based quadratic programs for safety critical systems," *IEEE Transactions on Automatic Control*, vol. 62, no. 8, pp. 3861–3876, 2017.

[9] Y. Meng, Y. Li, M. Fitzsimmons, and J. Liu, "Smooth converse Lyapunov-barrier theorems for asymptotic stability with safety constraints and reach-avoid-stay specifications," *Automatica*, vol. 144, p. 110478, 2022.

[10] B. G. Goswami, M. Tayal, K. Rajgopal, P. Jagtap, and S. Kolathaya, "Collision cone control barrier functions: Experimental validation on ugvs for kinematic obstacle avoidance," in *American Control Conference (ACC)*, 2024.

[11] C. P. Bechlioulis and G. A. Rovithakis, "Robust adaptive control of feedback linearizable MIMO nonlinear systems with prescribed performance," *IEEE Transactions on Automatic Control*, vol. 53, no. 9, pp. 2090–2099, 2008.

[12] C. P. Bechlioulis and G. A. Rovithakis, "A low-complexity global approximation-free control scheme with prescribed performance for unknown pure feedback systems," *Automatica*, vol. 50, no. 4, pp. 1217–1226, 2014.

[13] X. Bu, "Prescribed performance control approaches, applications and challenges: A comprehensive survey," *Asian Journal of Control*, vol. 25, no. 1, pp. 241–261, 2023.

[14] P. K. Mishra and P. Jagtap, "Approximation-free prescribed performance control with prescribed input constraints," *IEEE Control Systems Letters*, vol. 7, pp. 1261–1266, 2023.

[15] F. Chen and D. V. Dimarogonas, "Funnel-based cooperative control of leader-follower multi-agent systems under signal temporal logic specifications," in *European Control Conference*, pp. 906–911, 2022.

[16] F. Mehdifar, C. P. Bechlioulis, and D. V. Dimarogonas, "Funnel control under hard and soft output constraints," in *IEEE 61st Conference on Decision and Control*, pp. 4473–4478, 2022.

[17] L. Lindemann, C. K. Verginis, and D. V. Dimarogonas, "Prescribed performance control for signal temporal logic specifications," in *IEEE 56th Conference on Decision and Control*, pp. 2997–3002, 2017.

[18] H. Ravanbakhsh, S. Aghli, C. Heckman, and S. Sankaranarayanan, "Path-following through control funnel functions," in *IEEE/RSJ International Conference on Intelligent Robots and Systems*, pp. 401–408, 2018.

[19] R. Das and P. Jagtap, "Funnel-based control for reach-avoid-stay specifications," *arXiv preprint arXiv:2308.15803*, 2023.

[20] C. P. Bechlioulis, D. V. Dimarogonas, and K. J. Kyriakopoulos, "Robust control of large vehicular platoons with prescribed transient and steady state performance," in *53rd IEEE Conference on Decision and Control*, pp. 3689–3694, 2014.

[21] Y. Liu, X. Liu, and Y. Jing, "Adaptive neural networks finite-time tracking control for non-strict feedback systems via prescribed performance," *Information Sciences*, vol. 468, pp. 29–46, 2018.

[22] X. Bu, Y. Xiao, and K. Wang, "A prescribed performance control approach guaranteeing small overshoot for air-breathing hypersonic vehicles via neural approximation," *Aerospace Science and Technology*, vol. 71, pp. 485–498, 2017.

[23] H. Xu and P. Ioannou, "Robust adaptive control for a class of MIMO nonlinear systems with guaranteed error bounds," *IEEE Transactions on Automatic Control*, vol. 48, no. 5, pp. 728–742, 2003.

[24] E. D. Sontag, *Mathematical control theory: deterministic finite dimensional systems*, vol. 6. Springer Science and Business Media, 2013.

[25] MATLAB, *Navigation Toolbox version: 9.14 (R2023a)*. Natick, Massachusetts: The MathWorks Inc., 2024.

[26] S. M. LaValle, *Planning algorithms*. Cambridge university press, 2006.

[27] J. Xin, H. Zhao, D. Liu, and M. Li, "Application of deep reinforcement learning in mobile robot path planning," in *2017 Chinese Automation Congress (CAC)*, pp. 7112–7116, 2017.